Strain dependence of bonding and hybridization across the metal-insulator transition of VO_2

J. Laverock,[1] L. F. J. Piper,[1,2] A. R. H. Preston,[1] B. Chen,[1] J. McNulty,[1]
K. E. Smith,[1] S. Kittiwatanakul,[3] J. W. Lu,[4] S. A. Wolf,[3,4] P.-A. Glans,[5] and J.-H. Guo[5]

[1]*Department of Physics, Boston University, 590 Commonwealth Avenue, Boston, Massachussetts, MA 02215, USA*
[2]*Department of Physics, Applied Physics and Astronomy, Binghamton University, Binghamton, NY 13902, USA*
[3]*Department of Physics, University of Virginia, Charlottesville, VA 22904, USA*
[4]*Department of Materials Science and Engineering, University of Virginia, Charlottesville, VA 22904, USA*
[5]*Advanced Light Source, Lawrence Berkeley National Laboratory, Berkeley, California, CA 94720, USA*

arXiv:1202.2286v1 [cond-mat.str-el] 10 Feb 2012

Soft x-ray spectroscopy is used to investigate the strain dependence of the metal-insulator transition of VO_2. Changes in the strength of the V $3d$ - O $2p$ hybridization are observed across the transition, and are linked to the structural distortion. Furthermore, although the V-V dimerization is well-described by dynamical mean-field theory, the V-O hybridization is found to have an unexpectedly strong dependence on strain that is not predicted by band theory, emphasizing the relevance of the O ion to the physics of VO_2.

Of the materials that exhibit a metal-insulator transition (MIT), VO_2 has been an exquisite textbook example for the last five decades [1], with its large ($\sim 10^4$) discontinuity in the conductivity and the rich tunability of its properties with alloying or strain. Despite such intense interest, however, the nature of the transition itself still remains a challenge to explain. In the past, debate about whether the transition is driven by the lattice [2, 3] (Peierls physics) or by electron correlation effects [4, 5] (Mott-Hubbard physics) fuelled interest; more recently, the general consensus amongst experiment and theory alike is for a co-operative model, in which both pictures are important to the MIT. Key to understanding such a co-operative model has been the behavior of the transition with applied strain and alloying [5–8]. Technologically, interest in this material has focused on the dramatic changes of its optical properties through the transition, coupled with its ultra-fast nature [9], that make it an excellent candidate for applications such as fast optical switches.

The potential application of VO_2 as a novel functional material has recently been accelerated by advances in its thin film growth [10, 11], and such interest has been fuelled by the possibility of tailoring the MIT (including to below room temperature) through doping and/or strained thin films epitaxially grown on oriented TiO_2 substrates. However, the introduction of strain to the lattice (at ambient pressure) raises new questions on the physics of VO_2. In particular, the role of the lattice has important implications for the timescale of the transition, and many of the envisaged technological applications of VO_2 hinge on its ultra-fast nature. For example, the structural transition is known to impose a bottleneck on the timescale of the transition of bulk VO_2 [12]. Meanwhile, the effects of strain on the mechanism of the MIT are not well-established: in bulk VO_2, small amounts of applied uniaxial stress stabilize the M_2 phase [8], whereas for Nb-doped VO_2 (of Nb concentrations $\geq$ 15%) the chemical pressure induces an insulating rutile phase [4] (i.e. with no accompanying structural distortion). In this Letter, using a combination of soft x-ray spectroscopies, we show that the MIT of moderately strained VO_2 still involves the lattice, and reveal that the role of the O ion has a surprising dependence on the strain that is not anticipated by band theory.

The essential features of the electronic structure of VO_2 can be understood rather well from a simple molecular orbital perspective [2]. In this picture, the V $3d$ orbitals form three well-separated states in the high-temperature rutile (R) structure. Crucially, the π^* (also labeled e_g^π) states overlap in energy with the so-called $d_\parallel$ (a_{1g}) states that run along the rutile c-axis (c_R-axis), leading to a metallic phase. Accompanying the MIT, a structural distortion into the monoclinic M_1 phase leads to the dimerization of V atoms in the c_R-axis, splitting the $d_\parallel$ state into bonding and anti-bonding states. Additionally, the tilting of the VO_6 octahedra in the M_1 structure increases the V-O hybridization, and pushes the π^* state upwards in energy, deoccupying it and leading to an insulating phase. However, early measurements of the properties of Nb- and Cr-doped VO_2 [4, 5] revealed features of the phase diagram inconsistent with the neglect of electron correlations, e.g. an insulating rutile phase and the presence of the M_2 phase (in which only half the V atoms dimerize). In the model of Zylbersztejn and Mott [13], strong correlations in the $d_\parallel$ band are screened in the metallic phase by the π^* band. In the insulating phase, these π^* states are empty, and the unscreened correlations open the gap.

Attempts to describe the electronic structure from first-principles have had mixed success: the local density approximation (LDA) has not been able to account for the insulating phase, leading to a metallic solution for both R and M_1 structures [14]. On the other hand, the inclusion of static correlations in the LDA+U method correctly predict an insulating M_1 phase but cannot de-

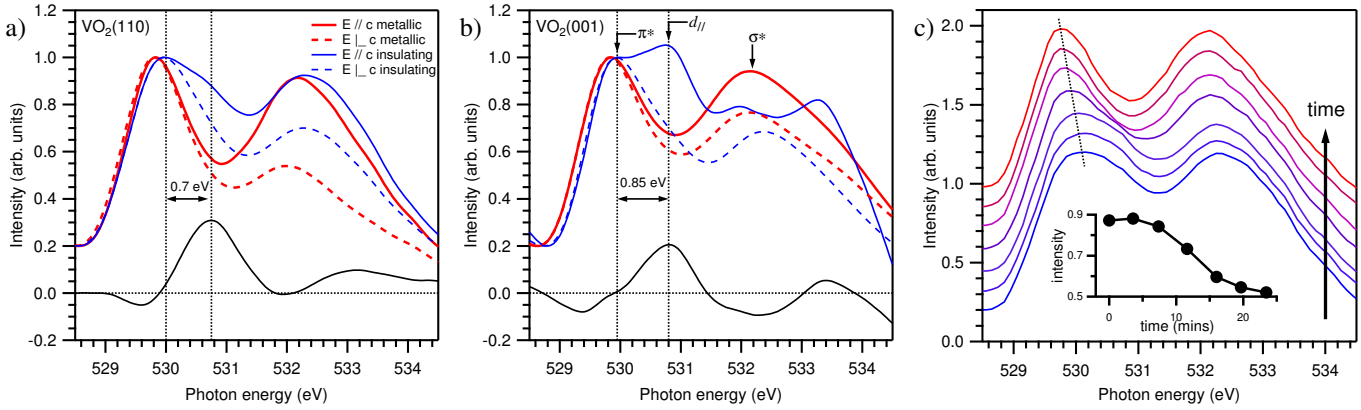

FIG. 1: (Color online) O K-edge XAS spectra for (a) VO_2(110) and (b) VO_2(001). Spectra are shown recorded both above (metallic) and below (insulating) the MIT with incident photons aligned parallel and perpendicular to the c_R-axis. At the bottom of each figure the difference between insulating and metallic spectra are shown. (c) O K-edge spectra recorded during a heating cycle through the transition for VO_2(110). The inset shows the evolution in intensity of the $d_{\|}$ peak.

scribe the R phase for reasonable values of U [15]. More recently, dynamical mean-field theory (DMFT) calculations [16, 17] and HSE hybrid functional calculations [18] have been able to describe both phases well.

X-ray spectroscopy is a powerful tool for addressing the electronic structure of complex materials, capable of revealing both the unoccupied and occupied site-specific partial density of states (PDOS) in the form of x-ray absorption spectroscopy (XAS) and x-ray emission spectroscopy (XES) respectively. Further, by rotating the polarization vector of the incident x-rays, it is possible to couple to orbitals of different symmetry. XAS measurements at the O K-edge of pure, bulk VO_2 [19] have revealed the main features of the unoccupied O $2p$ PDOS: peaks separated by ~ 2.5 eV in the metallic phase are related to the π^* and σ^* states. In the insulating phase, an additional peak owing to the $d_{\|}$ orbital develops at ~ 1 eV above π^*. More recent polarization-dependent measurements have unambiguously associated this peak with the $d_{\|}$ orbitals, demonstrating its presence when the polarization vector is parallel to the c_R-axis, and absence when it is perpendicular [20].

High-quality thin films (~ 40 nm) of VO_2 were grown on rutile TiO_2(110) and TiO_2(001) oriented substrates by reactive bias target ion-beam deposition [11]. X-ray diffraction measurements confirm the epitaxy of VO_2 with the substrate, and establish the contracted c_R-axis of VO_2 grown on TiO_2(001) compared with bulk, and expanded c_R-axis for VO_2 grown on TiO_2(110) [21]. In the following, *tensilely-strained* VO_2/TiO_2(110) is referred to as VO_2(110); correspondingly, *compressively-strained* VO_2/TiO_2(001) is referred to as VO_2(001). Soft x-ray spectroscopy measurements were carried out at beamline X1B of the National Synchrotron Light Source, Brookhaven and the AXIS endstation of beamline 7.0.1 at the Advanced Light Source, Berkeley. XAS measurements were made in total electron yield (TEY) mode with a beamline energy resolution of 0.2 eV at FWHM, and the photon energy was calibrated using TiO_2 reference spectra of the Ti L-edge and O K-edge. The XES spectra were recorded with a Nordgren-type spectrometer set to an energy resolution of 0.5 eV at FWHM, and the instrument was calibrated using a Zn reference spectrum.

In Fig. 1, we present O K-edge spectra for the two strained samples both above and below the MIT and for incident photon polarizations parallel and perpendicular to the c_R-axis. For the compressively strained VO_2(001) sample, whose $T_{MIT} \approx 300$ K, spectra were recorded in the metallic R phase at room temperature (RT) and insulating phase at ~ 100 K. Correspondingly, for the tensilely strained VO_2(110), with $T_{MIT} \approx 345$ K, data were recorded in the R phase at ~ 400 K and insulating phase at RT. For both samples, the spectra are in excellent qualitative agreement with the data of Refs. [19, 20]: in the metallic phase, two peaks are observed that correspond to the π^* and σ^* unoccupied states.

Turning our attention to the temperature dependence of the spectra, an additional peak ~ 1 eV above the π^* develops in the insulating phase for $E \parallel c_R$. The assignment of this peak as the $d_{\|}$ state that has previously been observed for bulk VO_2 [19, 20] is confirmed by its polarization dependence: it is absent in both samples for $E \perp c_R$. At the bottom of Fig. 1a,b, the difference between the insulating and metallic spectra for $E \parallel c_R$ is shown, highlighting the contribution from the $d_{\|}$ states. For compressive VO_2(001), the peak energy is found to be offset by 0.85 eV from the π^* band, close to the ~ 1 eV observed for bulk VO_2 [20]. On the other hand, for tensilely strained VO_2(110), the $d_{\|}$ peak shifts down in energy to 0.7 eV. These results are in good agreement with the strain-dependence of the $d_{\|}$ state from DMFT calculations, in which the offset between the π^* and $d_{\|}$ state are calculated to be 0.7 and 0.9 eV for tensive and compressive c_R-axis strain (each of 2% magnitude) respectively [17]. This observation of the unoccupied $d_{\|}$ band, and its dependence on strain, in the insulating phase of moderately strained VO_2 is evidence of a substantial V-V dimerizing structural distortion, similar to the M_1 or

M_2 phases of bulk VO_2. Factor analysis [22] of spectra recorded during a heating cycle through the transition (shown in Fig. 1c) revealed only two eigenvalues. The data were reproduced by a linear combination of the insulating and metallic end-members, supporting real-space measurements that suggest the absence of an intermediate phase and lack of dimerization above the MIT [23].

By resonantly exciting the system at an energy that corresponds to a feature in the XAS spectrum, it is possible to measure the site-selective occupied PDOS. In Fig. 2a the V L_3-edge resonant XES (RXES) spectra of the two samples in near-grazing geometry are shown above and below the MIT, and correspond to the fluorescent decay of occupied V 3d states to the empty V 2p core hole created in the excitation process (see Ref. [21] for details of the geometry of these measurements). Three principal features are observed in these spectra. Firstly, the peak at 0 eV is due to elastically scattered x-rays, whose intensity is found to vary with c_R-axis strain. Secondly, the feature centered at −4 eV represents a combination of fluorescence from occupied 'pure' V 3d orbitals, located just below E_F, and low-energy inelastic loss features. Although the separation of these two components is complicated by their proximity in energy, analysis of their angular dependence and comparison with photoemission measurements establish that the loss features are predominantly located below −3 eV. In fact, the strong kink in the VO_2(110) spectra at −3 eV separate the two components, analogous to the double-peaked structure observed for Mo-doped VO_2 [24]. Note that the double-peaked structure observed in our data has a different origin to that observed in photoemission measurements (see, for example, Refs. [20, 25]). Finally, the broader peak centered −9.5 eV represents V 3d states hybridized with O 2p states; the data presented in Fig. 2a have been normalized to this hybridized component. This interpretation is in agreement with other vanadates [26], including Cr-doped VO_2 [27].

Focusing first on the behavior of the spectra across the transition, both samples exhibit a substantial change in the ratio of the V 3d peak to the O 2p hybridized peak, with a stronger contribution from the pure V 3d states in the metallic R phase. Considering the occupation of the V 3d band to be approximately constant across the transition, this change in intensity is interpreted as an increase in the hybridization between O 2p and V 3d states in going from the metallic to the insulating phase. For $V_{1-x}Cr_xO_2$, a similar change in this ratio was observed as a consequence of Cr-doping, and was associated with the decrease in the lattice parameter [in particular, the $(110)_R$ lattice spacing] induced by Cr ion substitution [27]. For bulk rutile VO_2, the nearest-neighbor V-O distance is 1.92 Å. However, in the M_1 phase, the structural distortion (dimerization of V-V ions and particularly their associated twisting in the VO_6 octahedra) reduces this to 1.76 Å, substantially increasing the overlap of the V 3d and O 2p wave functions. Together with our XAS measurements, the RXES data establish that a

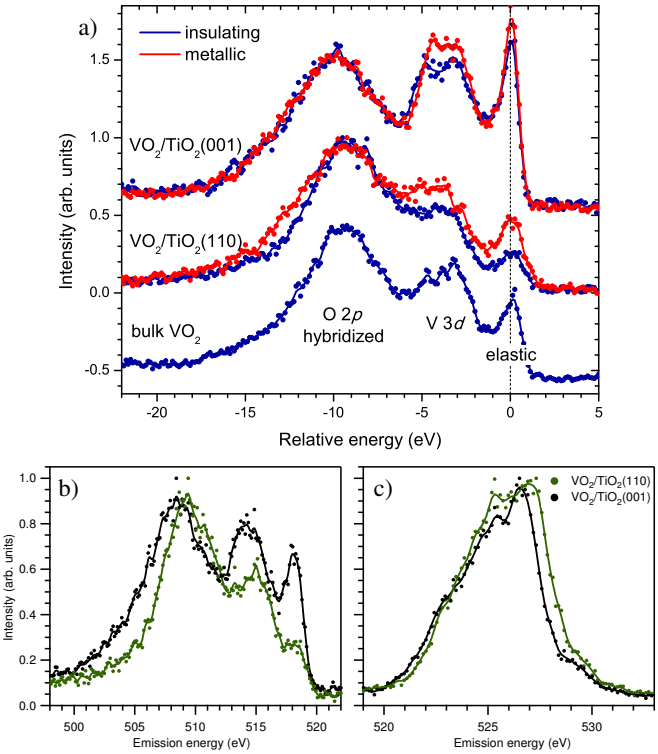

FIG. 2: (Color online) (a) RXES spectra of VO_2(110) and VO_2(001) above and below the MIT recorded at the V L_3-edge peak maximum. The spectrum of bulk M_1 VO_2 is also shown for comparison. The spectra have been normalized to the O 2p hybridized peak and are presented on an energy-loss scale and vertically offset. (b) V L_3-edge RXES and (c) O K-edge XES spectra of both samples at room temperature on a common emission energy axis.

structural distortion accompanies the MIT that increases the overlap between the V 3d and O 2p wave functions, in a similar manner to the M_1 or M_2 bulk phases.

Turning now to the behavior of the spectra as a function of strain, it is evident in Fig. 2a that there is a large change in the V 3d - O 2p hybridization between the two samples. Fig. 2b shows the RXES spectra on a common emission energy axis recorded *during the same measurement*, eliminating ambiguity in the energy calibration of the spectrometer. Firstly, the location of the O 2p (hybridized) feature is rigidly shifted upwards in energy by almost 1 eV for VO_2(110). Owing to the proximity of loss features, the shift of the V 3d PDOS is harder to accurately judge, but it is clear that any shift of these states is weaker. This indicates the V and O states are closer together in energy for VO_2(110), facilitating their enhanced hybridization. Indeed, this enhanced hybridization can be directly visualized in the data through the relative intensity of the O 2p hybridized feature compared with the V 3d peak. Qualitatively, such behavior can be understood from the evolution of the a_R-axis lattice parameter with strain. For VO_2(001), the a_R-axis is expanded, accommodating the strain, and the π-bonded V 3d and O 2p orbitals are pulled further apart, decreasing their

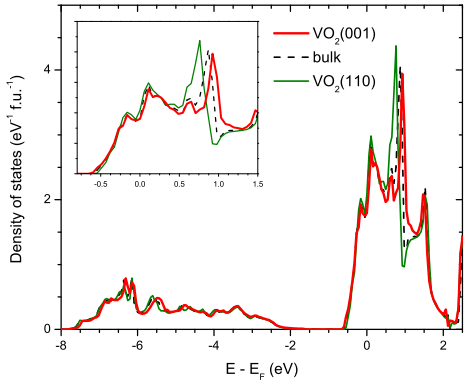

FIG. 3: (Color online) LDA partial V density of states of metallic rutile VO_2 for structures corresponding to the two strained systems investigated compared with bulk. Shown in the inset is an enlarged view of the V 3d t_{2g} states showing the evolution of the $d_{\|}$ peak with strain.

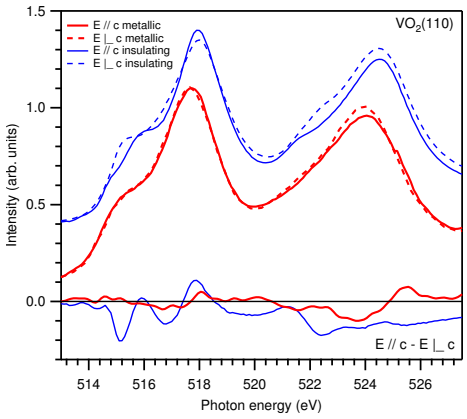

FIG. 4: (Color online) V $L_{3,2}$-edge XAS in both insulating and metallic phases, shown here for VO_2(110). At the bottom of the figure, the anisotropy of these spectra is shown.

respective hybridization. However, such strain-dependent changes in the hybridization between V and O states is not expected from band theory and hint towards a more significant role for the O ion than previously considered in the physics of the MIT of VO_2. Shown in Fig. 3 is the V PDOS within the LDA (employing the FLAPW Elk code [28]) of the metallic phase of both strained and bulk VO_2. The evolution of the $d_{\|}$ peak, shown in the inset, is in agreement with the LDA calculations of Ref. [17]. The energy axis in Fig. 2a refers to the excitation energy (rather than E_F), and the centroids of the calculated V-O and pure V states agree reasonably well with experiment with a rigid shift ~ 3 eV. However, the V-O hybridized states between -8 and -2 eV show only very weak dependence on the strain, both in relative intensity and energy, and certainly very much less than observed in our RXES measurements (Fig. 2a). An accurate model of the electronic structure of strained VO_2 must include such strain induced modifications to the O states of the electronic structure, not usually directly included in DMFT calculations.

O K-edge XES spectra are shown for the two samples in Fig. 2c and reflect the change in the local O 2p PDOS. Although there is a slight evolution in the low-energy onset of the spectra, the dominant difference is the appreciable narrowing of the bandwidth of VO_2(001). Whereas the O 2p feature of the RXES spectra recorded at the V L_3-edge are related to the hybridized portion of the O states, O K-edge XES spectra measure the total O 2p PDOS. In particular, the knee observed at ~ 529 eV has its origins in the mixing of the V 3d wavefunctions with O 2p character. The broader bandwidth of VO_2(110) is due to the enhanced hybridization with V 3d states, in agreement with the RXES data, and supported by the closer proximity, and indeed merging, of the knee to the onset of emission from the O 2p manifold.

Finally, in Fig. 4 the anisotropy of the V $L_{3,2}$-edge XAS spectra are shown above and below the MIT of VO_2(110); for this system, the splitting of the $d_{\|}$ state is more different (smaller) to that of bulk VO_2 (see Fig. 1). Below the transition, these spectra exhibit strong anisotropy, particularly at the V L_3-edge, which is suppressed in the metallic phase. This anisotropy has been previously associated with changes in the occupation of the V 3d orbitals for bulk VO_2 [29]. It is worth pointing out that electron correlations were required by Ref. [29] in order to explain their observations. These results demonstrate the same orbital switching occurs for moderately strained VO_2, requiring both the monoclinic structural distortion and the involvement of appreciable electron correlations.

In summary, complementary soft x-ray techniques have been employed to demonstrate (i) the evolution of V-V dimerization with strain (in excellent agreement with recent DMFT results), (ii) changes in the hybridization of V-O states across the MIT (related to the distortion of the VO_6 octahedra, and (iii) the orbital switching that occurs across the MIT. All of these results are consistent with the distorted monoclinic M_1 or M_2 low-temperature insulating phase. Finally, the V-O hybridization is found to have an unexpectedly strong dependence on strain, indicating a role for the O ion in the physics of the MIT of VO_2 that is often overlooked. We anticipate that these results will provide a stringent test of theoretical models of the properties of the MIT in strained VO_2.

Acknowledgements

We would like to thank S. Sallis for the factor analysis of our data. The Boston University program is supported in part by the Department of Energy under Grant No. DE-FG02-98ER45680. The ALS, Berkeley, is supported by the U.S. Department of Energy under Contract No. DE-AC02-05CH11231. The NSLS, Brookhaven, is supported by the U.S. Department of Energy under Contract No. DE-AC02-98CH10886. SK, JWL, SAW are thankful to the financial support from the Army Research Office through MURI grant No. W911-NF-09-1-0398.

[1] F. J. Morin, Phys. Rev. Lett. **3**, 34 (1959); N. F. Mott, *Metal-Insulator Transitions*, Taylor & Francis Ltd, London (1974).

[2] J. B. Goodenough and H. Y.-P. Hong, Phys. Rev. B **8**, 1323 (1973).

[3] E. Carruthers and L. Kleinman, Phys. Rev. B **7**, 3760 (1973).

[4] P. Lederer, H. Launois, J. P. Pouget, A. Casalot and G. Villeneuve, J. Phys. Chem. Solids **33**, 1969 (1972).

[5] J. P. Pouget, H. Launois, T. M. Rice, P. Dernier, A. Gossard, G. Villeneuve and P. Hagenmuller, Phys. Rev. B **10**, 1801 (1974).

[6] M. Marezio, D. B. McWhan, J. P. Remeika and P. D. Dernier, Phys. Rev. B **5**, 2541 (1972).

[7] G. Villeneuve, A. Bordet, A. Casalot, J. P. Pouget, H. Launois and P. Lederer, J. Phys. Chem. Solids **33**, 1953 (1972).

[8] J. P. Pouget, H. Launois, J. P. D'Haenens, P. Merenda and T. M. Rice, Phys. Rev. Lett. **35**, 873 (1975).

[9] A. Cavalleri, Cs. Tóth, C. W. Siders, J. A. Squier, F. Ráksi, P. Forget and J. C. Kieffer, Phys. Rev. Lett. **87**, 237401 (2001).

[10] Y. Muraoka and Z. Hiroi, Appl. Phys. Lett. **80**, 583 (2002).

[11] K. G. West, J. W. Lu, J. Yu, D. Kirkwood, W. Chen, Y. H. Pei, J. Claassen and S. A. Wolf, J. Vac. Sci. Technol. A **26**, 133 (2008).

[12] A. Cavalleri, Th. Dekorsy, H. H. W. Chong, J. C. Kieffer and R. W. Schoenlein, Phys. Rev. B **70**, 161102(R) (2004).

[13] A. Zylbersztejn and N. F. Mott, Phys. Rev. B **11** 4383 (1975).

[14] R. M. Wentzcovitch, W. W. Schulz and P. B. Allen, Phys. Rev. Lett. **72**, 3389 (1994); V. Eyert, Ann. Phys. (Leipzig) **11**, 650 (2002).

[15] M. A. Korotin, N. A. Skorikov and V. I. Anisimov, Phys. Met. Metallogr. **94**, 17 (2002); M. E. Williams, W. H. Butler, C.K. Mewes, H. Sims, M. Chshiev and S. K. Parker, J. Appl. Phys. **105**, 07E510 (2009).

[16] S. Biermann, A. Poteryaev, A. I. Lichtenstein and A. Georges, Phys. Rev. Lett. **94**, 026404 (2005).

[17] B. Lazarovits, K. Kim, K. Haule and G. Kotliar, Phys. Rev. B **81**, 115117 (2010).

[18] V. Eyert, Phys. Rev. Lett. **107**, 016401 (2011).

[19] M. Abbate, F. M. F. de Groot, J. C. Fuggle, Y. J. Ma, C. T. Chen, F. Sette, A. Fujimori, Y. Ueda and K. Kosuge, Phys. Rev. B **43**, 7263 (1991).

[20] T. C. Koethe, Z. Hu, M. W. Haverkort, C. Schüßler-Langeheine, F. Venturini, N. B. Brookes, O. Tjernberg, W. Reichelt, H. H. Hsieh, H.-J. Lin, C. T. Chen and L. H. Tjeng, Phys. Rev. Lett. **97**, 116402 (2006).

[21] See Supplemental Material for details of the sample growth and characterization, and of the anisotropy of the V L_3-edge RXES measurements.

[22] E. R. Malinowski, *Factor Analysis in Chemistry*, Wiley, New York (1991).

[23] S. A. Corr, D. P. Shoemaker, B. C. Melot and R. Seshadri, Phys. Rev. Lett. **105**, 056404 (2010).

[24] T. Schmitt, L.-C. Duda, M. Matsubara, A. Augustsson, F. Trif, J.-H. Guo, L. Gridneva, T. Uozumi, A. Kotani and J. Nordgren, J. Alloy Compd. **362**, 143 (2004).

[25] K. Okazaki, H. Wadati, A. Fujimori, M. Onoda, Y. Muraoka and Z. Hiroi, Phys. Rev. B **69**, 165104 (2004).

[26] T. Schmitt, L.-C. Duda, M. Matsubara, M. Mattesini, M. Klemm, A. Augustsson, J.-H. Guo, T. Uozumi, S. Horn, R. Ahuja, A. Kotani and J. Nordgren, Phys. Rev. B **69**, 125103 (2004); T. Schmitt, A. Augustsson, J. Nordgren, L.-C. Duda, J. Höwing, T. Gustafsson, U. Schwingenschlögl and V. Eyert, Appl. Phys. Lett. **86**, 064101 (2005).

[27] L. F. J. Piper, A. DeMasi, S. W. Cho, A. R. H. Preston, J. Laverock, K. E. Smith, K. G. West, J. W. Lu and S. A. Wolf, Phys. Rev. B **82**, 235103 (2010).

[28] J. K. Dewhurst, S. Sharma, L. Nordstöm, F. Cricchio and F. Bultmark, `http://elk.sourceforge.net` (2009).

[29] M. W. Haverkort, Z. Hu, A. Tanaka, W. Reichelt, S. V. Streltsov, M. A. Korotin, V. I. Anisimov, H. H. Hsieh, H.-J. Lin, C. T. Chen, D. I. Khomskii and L. H. Tjeng, Phys. Rev. Lett. **95**, 196404 (2005).